

# SUPPLEMENTAL MATERIAL

## Methods

### *Plasmids and heterologous expression*

Human KCNQ1 and KCNE1 cDNAs were generated as described previously.<sup>1</sup> The S140G and V141M mutations were engineered in KCNQ1 using QuikChange mutagenesis (Stratagene Corp, La Jolla, CA). For experiments comparing heteromeric channel complexes consisting of only one KCNQ1 allele, cells were transiently transfected with KCNE1-IRES2-eGFP and either KCNQ1-IRES2-DsRedMST (WT-I<sub>Ks</sub>) or S140G-IRES2-DsRedMST (S140G-I<sub>Ks</sub>). For expression of V141M-I<sub>Ks</sub>, cells were co-transfected with KCNE1-IRES2-DsRedMST and V141M-IRES2-eGFP plasmids. To study heteromeric channel complexes with both WT and mutant (S140G) KCNQ1 subunits, WT-I<sub>Ks</sub> was expressed in cells transfected with KCNE1-IRES2-CD8, KCNQ1-IRES2-eGFP and KCNQ1-IRES2-DsRedMST whereas HET-I<sub>Ks</sub> was reconstituted by transfecting cells with KCNE1-IRES2-CD8, KCNQ1-IRES2-eGFP and S140G-IRES2-DsRedMST. The efficiency of triple transfection was approximately 1-5%. All constructs were verified by sequencing of the entire open reading frames.

Chinese hamster ovary cells (CHO-K1, American Type Culture Collection, Manassas, VA) were grown at 37°C with 5% CO<sub>2</sub> in F-12 nutrient mixture medium supplemented with 10% fetal bovine serum (FBS, Atlanta Biologicals, Atlanta, GA), penicillin (50 units/ml), streptomycin (50 µg/ml), and L-glutamine (2 mM). Unless otherwise stated, all tissue culture media were obtained from Life Technologies (Grand Island, NY). CHO cells were transiently transfected using FuGENE 6 (Roche Applied Sciences, Indianapolis, IN) at a ratio of 3:1.

### *Adenovirus generation*

Adenovirus vectors, pAd5-CMVK-NpA and pAd5-(9.2-100)delta1.6KbE3, were obtained from the University of Iowa Gene Transfer Vector Core (supported in part by the NIH and the Roy J. Carver Foundation). Using the pAd5-CMVK-NpA vector, we created shuttle vectors for KCNQ1-IRES2-DsRedMST, S140G-IRES2-DsRedMST, and KCNE1-IRES2-eGFP. A modified CMV promoter was used for all shuttle vectors. This modified promoter consisted of the CMV immediate early promoter sequence immediately followed by last 358 nucleotides of IRES2. This modification was hypothesized to attenuate promoter efficiency and enabled more efficient generation of KCNQ1 encoding adenovirus.

Adenovirus was generated using the RAPAd™ system as previously described.<sup>2</sup> In brief, each shuttle vector and the backbone vector pAd5-(9.2-100)delta1.6KbE3 were co-precipitated with calcium-chloride into human embryonic kidney (HEK) 293 cells in 60 mm Petri dishes. When 60% of cells had detached (12-14 days for KCNE1 and vector-only viruses; 17-25 days for KCNQ1 and S140G), the cells and media were harvested, lysed through repeated freezing/thawing cycles, and amplified in HEK cells (typically using 5-10 150 mm Petri dishes). After 60% of cells detached from the large dishes (1-3 days), cells were pelleted by centrifugation and resuspended 5 ml of viral storage solution (10 mM Tris, 2 mM MgCl<sub>2</sub>, 4% sucrose, pH 8.0). Cells were then lysed and centrifuged. The supernatant was stored at -80°C in single use aliquots and the virus was used within 5 months.

Viral titer was determined using the tissue culture infective dose 50 (TCID<sub>50</sub>) method as described for the AdenoVator™ Vector System (QBioGene, Carlsband, CA). For multiplicity of infection (MOI) calculations, titers were converted to plaque forming units (PFU) by the following equation: PFU = 0.69\*TCID<sub>50</sub>. The titers achieved ranged from 10<sup>9</sup> to 10<sup>10</sup> PFU/ml. Activity of each virus prep was confirmed for fluorescent marker and potassium channel expression by

transduction and subsequent whole cell patch clamp of CHO cells stably expressing the coxsackie adenovirus receptor (CHO-CAR cells), generously provided by Dr. Jeffrey Bergelson at the University of Pennsylvania.<sup>3</sup>

#### *Rabbit atrial myocyte isolation*

Left atrial myocytes were isolated from hearts of male New Zealand White rabbits (6-7 lbs from Charles River Canada), using the method of Bassani, *et al.*<sup>4</sup> with modifications. Briefly, rabbits were sedated with intramuscular acepromazine and then anesthetized with intravenous pentobarbital sodium. Hearts were excised quickly and arrested on ice for 5 minutes in nominally calcium-free minimum essential medium solution (MEM, Joklik modification). Hearts were Langendorff perfused at 37°C for 10-15 min in the same MEM solution gassed with 95% O<sub>2</sub> and 5% CO<sub>2</sub>. During initial perfusion, the pulmonary vessels were closed with microvessel clips to perfuse both atrial chambers at high pressure, and the atrial chambers were punctured twice at their apex to facilitate flow-through. Then the perfusion was switched to MEM solution containing 0.05 mg/ml Liberase TH (Roche Applied Sciences). After 5 min of enzymatic digestion, a small incision was made in the left ventricle in an area between major coronary vessels. Serial tissue samples (30 s - 1 min) were taken from this incision with fine tweezers and inspected immediately by light microscopy. When the majority of ventricular myocytes released were quiescent rods (7-20 min), the left atrium was removed from the heart, the remaining heart was removed from the Langendorff apparatus, and left atrium was recannulated on the Langendorff apparatus. Serial samples were taken from the perfused atrium until the sample edges contained packets of rod-shaped atrial myocytes and the majority of released atrial myocytes were quiescent rods (5-20 minutes). The left atrium was removed and placed in MEM solution containing 1% bovine serum albumin (BSA). The tissue was minced, gently triturated with a wide-bore pipette, and filtered through a 100 µm cell strainer (BD Biosciences, San Jose, CA) into a 50 ml conical tube. The myocytes were allowed to settle into a soft pellet

by gravity for 30 – 60 min at room temperature. Then the supernatant was aspirated, and atrial myocytes were resuspended in fresh BSA solution. Myocytes were plated on laminin-coated glass coverslips, and incubated at 37°C with 5% CO<sub>2</sub>. The experimental procedure for isolating rabbit cardiac myocytes was approved by Vanderbilt University Institutional Animal Care and Use Committee.

#### *Atrial myocyte culture and adenoviral transduction*

Three hours after termination of enzymatic digestion, myocytes were placed into culture media consisting of MEM supplemented with Hank's salts, 2 mM L-glutamine (Gibco-Invitrogen), insulin-transferrin-selenium-X supplement (Gibco-Invitrogen), penicillin (50 units/ml), streptomycin (50 µg/ml), 1% bovine serum albumin, 5 µM blebbistatin at pH 7.4 (modified from Kabaeva, *et al.*<sup>5</sup>). Virus was added to the myocytes at a MOI of 2,000 immediately after plating in culture media. To express WT-I<sub>Ks</sub>, adenoviruses Ad5-KCNQ1-DsRedMST and Ad5-KCNE1-eGFP were used to co-infect myocytes, whereas S140G-I<sub>Ks</sub> was generated by co-infecting myocytes with adenoviruses Ad5-S140G-DsRedMST and Ad5-KCNE1-eGFP. Infected myocytes were cultured at 37°C in 5% CO<sub>2</sub> and used for electrophysiology experiments 48-72 hours post-isolation. The efficiency of dual transduction of healthy-appearing (striated, rod-shaped) myocytes was approximately 15-20%.

#### *Voltage clamp recording*

Potassium currents were recorded from CHO cells using the whole-cell configuration of the patch clamp technique.<sup>6</sup> In dual transfection experiments examining channels composed of KCNE1 with just one KCNQ1 allele, only cells exhibiting yellow fluorescence (co-expression of dsRed-MST and eGFP) were studied. In triple transfection experiments designed to examine heteromeric channels composed of KCNE1 with both WT and mutant KCNQ1 subunits, yellow fluorescent cells with at least 3 adhered anti-CD8 Dynabeads<sup>®</sup> (Life Technologies, Grand

Island, NY) were studied. The extracellular solution contained in mM: 132 NaCl, 4.8 KCl, 1.2 MgCl<sub>2</sub>, 1 CaCl<sub>2</sub>, 5 glucose, and 10 HEPES, pH 7.4. In experiments with drug application, bath solution containing vehicle (<0.01% dimethyl sulfoxide) or HMR-1556 (1 nM - 2 μM) was applied by pencil perfusion using the Automate Valve-link perfusion system. HMR-1556 ((3R,4S)-(+)-N-[3-hydroxy-2,2-dimethyl-6-(4,4,4-trifluorobutoxy)chroman-4-yl]-N-methyl-ethanesulfonamide) was synthesized by the Vanderbilt Institute of Chemical Biology Synthesis Core using a published method.<sup>7</sup> The standard intracellular solution contained in mM: 110 potassium aspartate, 1 CaCl<sub>2</sub>, 10 HEPES, 11 EGTA, 1 MgCl<sub>2</sub>, and 5 K<sub>2</sub>ATP, pH 7.35. Pipette solution was diluted 5-10% to prevent activation of swelling-activated currents. Patch pipettes were pulled from thick wall borosilicate glass (World Precision Instruments, Inc.) with a multistage P-97 Flaming-Brown micropipette puller (Sutter Instrument Co., Novato, CA) and heat-polished with a Micro Forge MF 830 (Narashige International USA, Inc., East Meadow, NY). After heat polishing, the resistance of the patch pipettes was 2-4 megaohms in the standard solutions. A 2% agar bridge with composition similar to the control bath solution was used as a reference electrode. Unless otherwise stated, all chemicals were obtained from Sigma-Aldrich (St. Louis, MO).

Whole-cell currents were recorded at room temperature (20–23°C) using an Axopatch 200B amplifier (MDS Analytical Technologies, Sunnyvale, CA). Test pulses were generated using Clampex 8.1 (MDS Analytical Technologies), and whole-cell currents were acquired at 5 kHz and filtered at 1 kHz. The access resistance and apparent membrane capacitance were estimated as described previously.<sup>8</sup> Whole-cell currents were not leak subtracted. Junction potentials were zeroed with the filled pipette in the bath solution. All recordings were started 4 min after achieving a whole cell patch. For concentration-response experiments, a single 2 s pulse to +40mV from a holding potential of -80 mV followed by a 1 s voltage step to -30mV

was repeated every 10 s. Following 30 s of stable current levels, HMR-1556 was applied until 1 min of steady-state current was observed. For activation protocols, whole-cell currents were measured during a series of 2 s voltage steps from a holding potential of -80 mV to test potentials ranging from -80 to +60 mV (in 10 mV increments) followed by a 1 s step to -30 mV to record tail currents with a 20 s interpulse duration. For current accumulation experiments, a single 2 s pulse to +40 mV followed by a 1 s step to -30mV was repeated for 1 minute with a 1 s interpulse duration.

### *Voltage clamp data analysis*

Data were collected for each experimental condition from at least three separate transfections and analyzed using a combination of Clampfit (MDS Analytical Technologies), OriginPro 7 (OriginLab Corp., Northampton, MA), and SigmaPlot 2000 (Systat Software, Inc., Chicago, IL). To determine the kinetics of onset of and recovery from inhibition, fractional current remaining over time after 1  $\mu$ M HMR-1556 application or after wash with bath solution was fitted with a monoexponential function ( $f(t) = \sum_{i=1}^n A_i e^{-\frac{t}{\tau_i}} + C$ ) where  $t$  indicates time,  $\tau$  is a time constant,  $A$  is an amplitude term and  $C$  is the fraction of unblocked current. The  $IC_{50}$  for inhibition of WT- $I_{Ks}$  was determined by fitting the percent inhibition from 1 nM to 2  $\mu$ M HMR-1556 with  $y = I_{min} + (I_{max} - I_{min}) / (1 + 10^{\log(IC_{50}) - x} * k)$  for monophasic fits where  $I_{min}$  is the minimal current inhibition,  $I_{max}$  is the maximal current inhibition,  $IC_{50}$  is the concentration producing half maximal inhibition,  $x$  is log of concentration, and  $k$  is the Hill slope factor.

For biphasic fits required for S140G- $I_{Ks}$ , V141M- $I_{Ks}$  and HET- $I_{Ks}$ , we used  $y = I_{min} + (I_{maxA} - I_{min}) / (1 + 10^{(x - IC_{50A}) * kA}) + (I_{maxB} - I_{min}) / (1 + 10^{(IC_{50B} - x) * kB})$  where  $I_{maxA}$  and  $I_{maxB}$  are the maximal current inhibition for the high and the low affinity states, respectively,  $IC_{50A}$  and  $IC_{50B}$  are the concentrations that produce half maximal inhibition of the high or low affinity states, respectively,  $kA$  and  $kB$  are the Hill slope factors for the high and low affinity states,

respectively. Instantaneous current was measured 100 ms following a voltage step and steady-state current was measured at 1900 ms. Current density was obtained by normalizing current level to cell capacitance. Voltage dependence of activation was determined by plotting normalized peak tail current versus voltage, then fitting curves with a Boltzmann function to determine the voltage for half-maximal activation ( $V_{1/2}$ ) and the slope factor ( $k$ ). Deactivation time constants were determined by fitting tail current decay with the monoexponential function shown above.

Differences between two groups were assessed using unpaired Student's *t* test. When comparing more than two groups, one-way ANOVA followed by a Tukey post hoc test was performed on values obtained for a given membrane voltage. Statistical tests were performed using SigmaStat 2.03 (Systat Software, Inc., Chicago, IL). Significance levels are reported as two-sided *p*-values.

#### *Current clamp recording*

Action potentials were elicited from atrial myocytes using the whole-cell configuration of the patch clamp technique.<sup>6</sup> Yellow, striated atrial myocytes were used for patch clamp experiments using previously described solutions.<sup>9</sup> The extracellular solution contained in mM: 140 NaCl, 5.4 KCl, 1 MgCl<sub>2</sub>, 1 CaCl<sub>2</sub>, 7.5 glucose, 0.33 NaH<sub>2</sub>PO<sub>4</sub>, and 5 HEPES, pH 7.4. The intracellular solution contained in mM: 120 KCl, 10.25 NaCl, 5 MgCl<sub>2</sub>, 0.36 CaCl<sub>2</sub>, 5 HEPES, 5 EGTA, 5 creatine phosphate (Tris), 5 glucose, and 5 K<sub>2</sub>ATP, pH 7.2. For drug application, bath solution containing vehicle (<0.01% dimethyl sulfoxide) or HMR-1556 (1 μM) was applied by pencil perfusion using the Automate Valve-link perfusion system. Patch pipettes were pulled from thick wall borosilicate glass (World Precision Instruments, Inc., Sarasota, FL) with a multistage P-97 Flaming-Brown micropipette puller (Sutter Instrument Co., Novato, CA) and heat-polished with a Micro Forge MF 830 (Narashige International USA, Inc., East Meadow, NY). After heat

polishing, the resistance of the patch pipettes was 1.5-2.5 megaohms in the above solutions. A 2% agar bridge with composition similar to the control bath solution was used as a reference electrode.

Action potentials were elicited at room temperature (20–23°C) using an Axopatch 700B amplifier (MDS Analytical Technologies, Sunnyvale, CA). Pulses were generated using Clampex 9.1 (MDS Analytical Technologies), and action potentials were acquired at 10 kHz. No current was injected to maintain resting membrane potentials. To elicit action potentials, a stimulus threshold was determined for each myocyte, using a protocol of 0.1 nA steps of 3-4 ms duration. For experiments, 1.25 times stimulus threshold was used. Action potentials were elicited at 0.1 Hz for 5 min initially to achieve equilibration, and then at 1 Hz for experiments. HMR-1556 was applied after steady state action potential duration (APD) was achieved.

#### *Current clamp data analysis*

Data were collected for each experimental condition from at least three separate myocyte isolations and analyzed using a combination of Clampfit 9.1 (MDS Analytical Technologies) and Excel 2010 (Microsoft). Data were transferred from Clampfit to Excel with each 1 Hz recording period contained in a separate file. A Visual Basic for Applications (VBA) program in Excel was written to read each file and to determine the resting membrane potential and atrial action potential duration at 90% (APD<sub>90</sub>) for each recorded action potential. The resting membrane potential (RMP) in mV was defined as the average value observed 10 ms prior to the stimulus. APD<sub>90</sub> was defined as time from the action potential overshoot to the return to 90% RMP. The overshoot was defined as the highest value after the current stimulus. All parameters determined were placed in a new Excel file organized by recording file name and trace number. To assess accuracy, parameters for randomly selected action potentials in each recording were verified manually using Clampfit. For each experimental condition, the



parameters were averaged for the last 10 recorded action potentials. Differences between two groups were assessed using unpaired Student's  $t$  test. Statistical tests were performed using SigmaStat 2.03 (Systat Software, Inc.).

## SUPPLEMENTAL REFERENCES

1. Lundquist AL, Manderfield LJ, Vanoye CG, Rogers CS, Donahue BS, Chang PA, Drinkwater DC, Murray KT, George AL, Jr. Expression of multiple KCNE genes in human heart may enable variable modulation of  $I_{Ks}$ . *J Mol Cell Cardiol.* 2005;38:277-287.
2. Anderson RD, Haskell RE, Xia H, Roessler BJ, Davidson BL. A simple method for the rapid generation of recombinant adenovirus vectors. *Gene Ther.* 2000;7:1034-1038.
3. Bergelson JM, Cunningham JA, Droguett G, Kurt-Jones EA, Krithivas A, Hong JS, Horwitz MS, Crowell RL, Finberg RW. Isolation of a common receptor for Coxsackie B viruses and adenoviruses 2 and 5. *Science.* 1997;275:1320-1323.
4. Bassani JW, Bassani RA, Bers DM. Calibration of indo-1 and resting intracellular [Ca]<sub>i</sub> in intact rabbit cardiac myocytes. *Biophys J.* 1995;68:1453-1460.
5. Kabaeva Z, Zhao M, Michele DE. Blebbistatin extends culture life of adult mouse cardiac myocytes and allows efficient and stable transgene expression. *Am J Physiol Heart Circ Physiol.* 2008;294:H1667-H1674.
6. Hamill OP, Marty A, Neher E, Sakmann B, Sigworth FJ. Improved patch-clamp techniques for high-resolution current recording from cells and cell-free membrane patches. *Pflügers Arch.* 1981;391:85-100.
7. Gerlach U, Brendel J, Lang HJ, Paulus EF, Weidmann K, Bruggemann A, Busch AE, Suessbrich H, Bleich M, Greger R. Synthesis and activity of novel and selective  $I_{Ks}$ -channel blockers. *J Med Chem.* 2001;44:3831-3837.
8. Lindau M, Neher E. Patch-clamp techniques for time-resolved capacitance measurements in single cells. *Pflügers Arch.* 1988;411:137-146.
9. Liu GX, Choi BR, Ziv O, Li W, de LE, Qu Z, Koren G. Differential conditions for early after-depolarizations and triggered activity in cardiomyocytes derived from transgenic LQT1 and LQT2 rabbits. *J Physiol.* 2012;590:1171-1180.

## SUPPLEMENTAL FIGURES

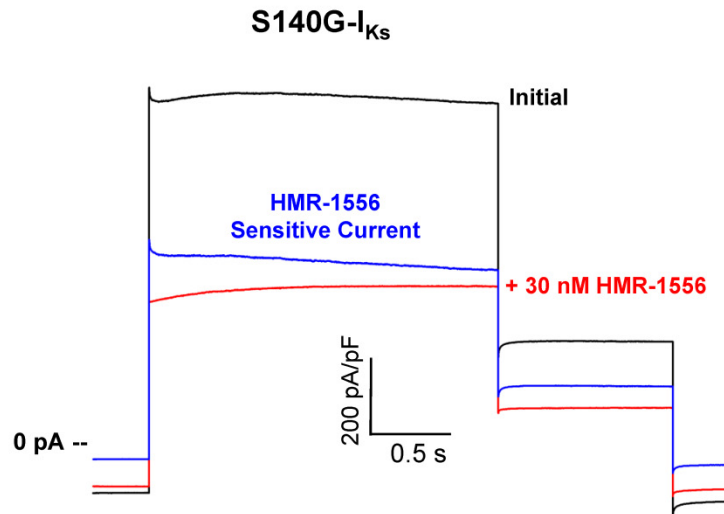


**Figure S1.** Average current densities for S140G-I<sub>Ks</sub> recorded in the absence (black trace) or presence (red trace) of 30 nM HMR-1556. HMR-1556 sensitive current (blue trace) was determined by digitally subtracting the residual current (red trace) from the total current (black trace).

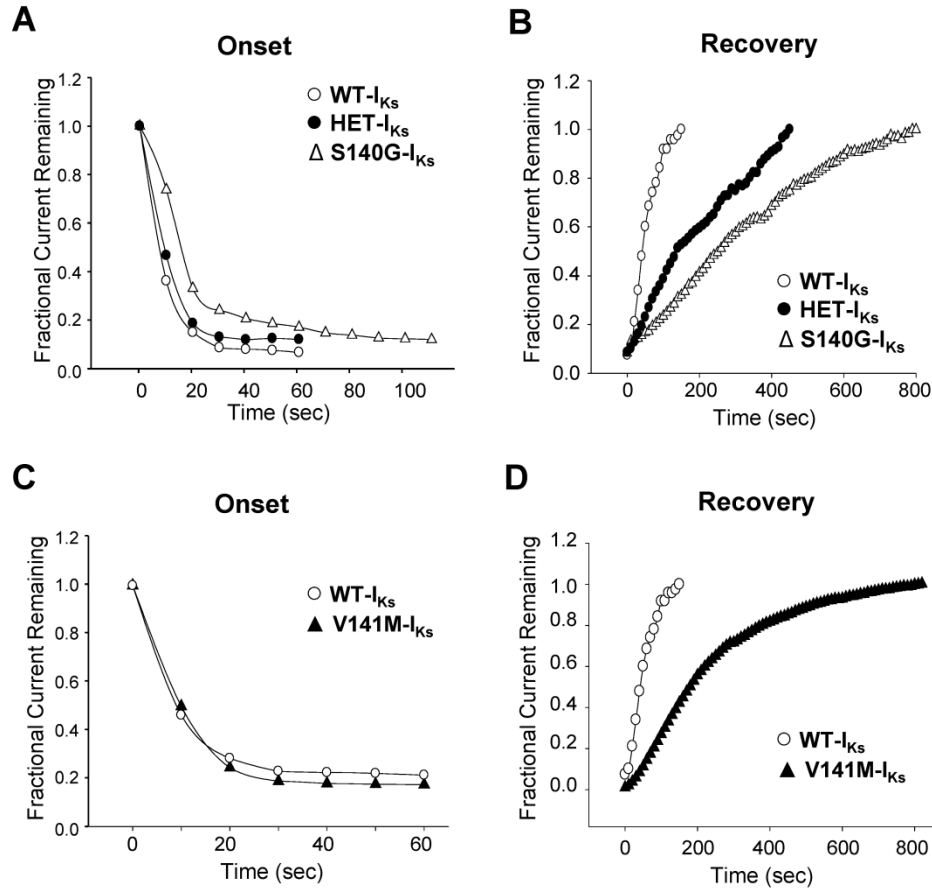


**Figure S2.** Kinetics of inhibition by HMR-1556. **A**, Onset of inhibition elicited by application of 1  $\mu\text{M}$  HMR-1556 for WT- $I_{Ks}$  ( $\circ$ ), S140G- $I_{Ks}$  ( $\Delta$ ), and HET- $I_{Ks}$  ( $\bullet$ ) illustrated for representative cells. On rates: WT- $I_{Ks}$ ,  $0.10 \pm 0.01 \text{ sec}^{-1}$ ; S140G- $I_{Ks}$ ,  $0.032 \pm 0.005 \text{ sec}^{-1}$ ; HET- $I_{Ks}$ ,  $0.12 \pm 0.01 \text{ sec}^{-1}$ . Differences between on rates were significant ( $p < 0.001$ ) for S140G- $I_{Ks}$  compared to HET- $I_{Ks}$  and WT- $I_{Ks}$ . **B**, Recovery from inhibition by 1  $\mu\text{M}$  HMR-1556 for WT- $I_{Ks}$  ( $\circ$ ), S140G- $I_{Ks}$  ( $\Delta$ ) and HET- $I_{Ks}$  ( $\bullet$ ) illustrated for representative cells. Off rates: WT- $I_{Ks}$ ,  $0.018 \pm 0.001 \text{ sec}^{-1}$ ; S140G- $I_{Ks}$ ,  $0.0020 \pm 0.0001 \text{ sec}^{-1}$ ; HET- $I_{Ks}$ ,  $0.0048 \pm 0.0009 \text{ sec}^{-1}$ . Differences were significant ( $p < 0.001$ ) for HET- $I_{Ks}$  and S140G- $I_{Ks}$  compared to WT- $I_{Ks}$ ; **C**, Onset of inhibition elicited by application of 1  $\mu\text{M}$  HMR-1556 for V141M- $I_{Ks}$  ( $\blacktriangle$ ) illustrated for representative cells. WT- $I_{Ks}$  ( $\circ$ ) shown for reference. The on rate observed for V141M- $I_{Ks}$ ,  $0.09 \pm 0.02 \text{ sec}^{-1}$ , was not significantly different ( $p = 0.28$ ) from that of WT- $I_{Ks}$ . **D**, Recovery from inhibition by 1  $\mu\text{M}$  HMR-1556 for V141M- $I_{Ks}$  ( $\blacktriangle$ ) illustrated for representative cells with WT- $I_{Ks}$  ( $\circ$ ) shown for reference. The off rate for V141M- $I_{Ks}$ ,  $0.004 \pm 0.002 \text{ sec}^{-1}$ , was significantly different ( $p < 0.001$ ) from WT- $I_{Ks}$ . In **A-D**, the data represent the current amplitude recorded at 1990 ms after a test pulse to +40 mV and normalized to current recorded at the initial pulse ( $n = 4-7$ ).

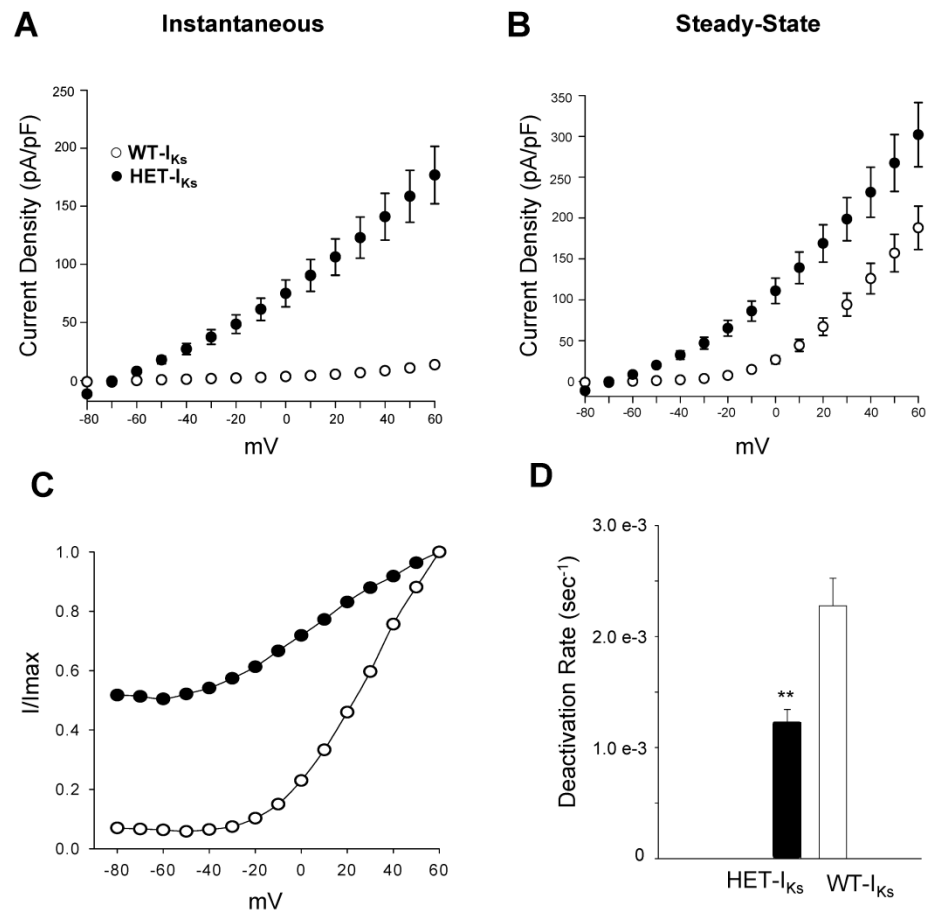


**Figure S3.** Functional properties of Het- $I_{Ks}$ . **A**, Voltage dependence of instantaneous current density recorded 100 ms after onset of the voltage step for WT- $I_{Ks}$  ( $\circ$ ,  $n = 19$ ) and HET- $I_{Ks}$  ( $\bullet$ ,  $n = 19$ ). Differences were significant at the  $p < 0.001$  level for voltages between  $-60$  and  $+60$  mV. **B**, Voltage dependence of steady-state current density recorded 1990 ms after onset of the voltage step for WT- $I_{Ks}$  ( $\circ$ ) and HET- $I_{Ks}$  ( $\bullet$ ). Current densities are significantly different ( $p < 0.02$ ) between WT- $I_{Ks}$  and HET- $I_{Ks}$  at all voltages except  $-70$  mV (reversal potential). **C**, Voltage dependence of activation for WT- $I_{Ks}$  ( $\circ$ ,  $n = 16$ ) and HET- $I_{Ks}$  ( $\bullet$ ,  $n = 13$ ). Solid lines represent average of Boltzmann fits to data from individual cells. Values for slope factor were not different between WT- $I_{Ks}$  ( $16.9 \pm 0.6$ ) and HET- $I_{Ks}$  ( $20.9 \pm 3$ ). Values for  $V_{1/2}$  are provided in the text. **D**, Deactivation kinetics illustrated for WT- $I_{Ks}$  ( $n = 9$ ) and HET- $I_{Ks}$  ( $n = 11$ ). Tail currents were elicited by a 2 s test pulse to  $+40$  mV from a holding potential of  $-80$  mV followed by sequential 2 s test pulses from  $-40$  mV to  $-100$  mV in 10 mV increments. At  $-100$  mV, HET- $I_{Ks}$  has a significantly slower deactivation rate than WT- $I_{Ks}$  ( $1.22e-3 \pm 0.11e-3$ , vs.  $2.28e-3 \pm 0.25e-3$ ;  $p < 0.02$ ).

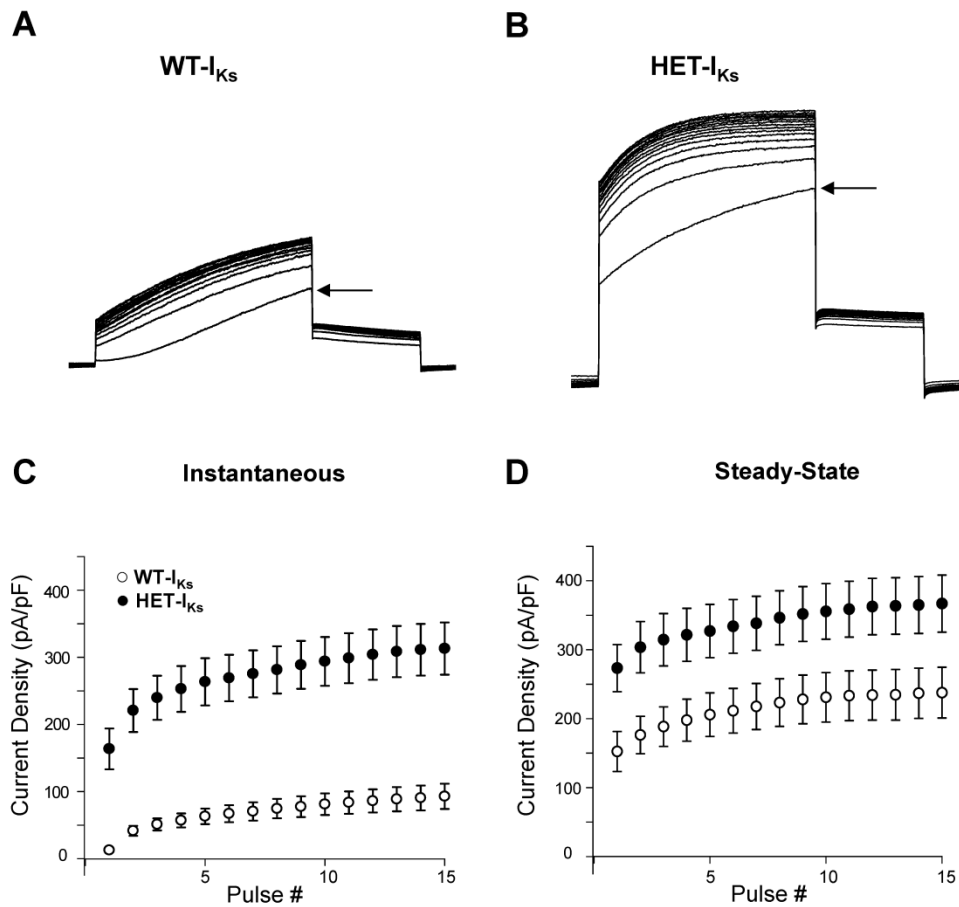


**Figure S4.** HET- $I_{Ks}$  exhibits use-dependent current accumulation. **A and B**, Representative current recordings during repetitive pulsing from cells expressing WT- $I_{Ks}$  (**A**) or HET- $I_{Ks}$  (**B**). For **A** and **B**, cells were repetitively depolarized to +40 mV for 2 s and then to -30 mV for 1 s followed by a 1 s interpulse interval at the holding potential. The first pulse is indicated by the arrow. **C**, Use dependence of instantaneous current density for cells expressing WT- $I_{Ks}$  ( $\circ$ ,  $n = 13$ ) and HET- $I_{Ks}$  ( $\bullet$ ,  $n = 14$ ). Differences were significant at the  $p < 0.001$  level for all pulses. **D**, Use dependence of steady-state current density for WT- $I_{Ks}$  ( $\circ$ ) and HET- $I_{Ks}$  ( $\bullet$ ) expressing cells. Differences were significant at the  $p < 0.03$  level for all pulses.

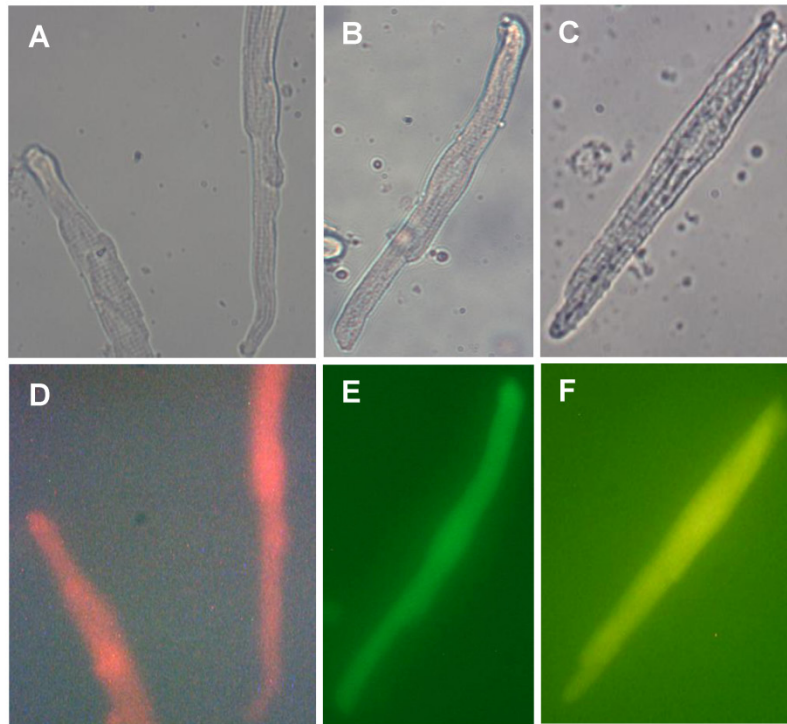


**Figure S5.** Adenoviral transduction of adult rabbit left atrial myocytes after 52 hours in culture. Representative bright field (**A-C**) and fluorescent (**D-F**) images of the same atrial myocytes. Myocytes were transduced with Ad-S140G-dsRedMST (**A,D**), Ad-KCNE1-eGFP (**B,E**), or both Ad-S140G-dsRedMST and Ad-KCNE1-eGFP (**C,F**).